

RESEARCH

Open Access



Integrative analysis of serum proteomics and transcriptomics in hepatitis C

Jianqiong Wang^{1†}, Andong Xia^{2†}, Min Tang¹, Shengjun Yang¹, Yandi Shen¹, Jinhua Dao¹, Rui Tao^{1*} and Wei Yue^{2*}

Abstract

Object Hepatitis C is a contagious disease caused by infection with the hepatitis C virus (HCV) through blood and mother-to-child routes. This study intends to characterize the serum molecular features of hepatitis C using proteomics and transcriptomics.

Methods Ctrl (normal population), HCV (population with previous HCV infection), and chronic HCV (patients with persistent HCV infection) groups were set up, and the expression profiles of the proteomes and transcriptomes of serum samples were identified using TMT and RNA-seq. Bioinformatics was applied to perform enrichment analysis and PPI network construction of differentially expressed proteins/genes (DEPs/DEGs). RT-qPCR and western blot verified the expression differences of DEPs/DEGs.

Results Compared to the Ctrl group, the HCV group had 356 DEPs in serum; compared to the HCV group, the chronic HCV group had 381 DEPs in serum. DEPs are predominantly immunoglobulins and exosomal proteins that regulate carbon dioxide transport, initiation of transcription, immune responses, and bacterial and viral infections. HSPA4, HSPD1, COPSS5, PSMD2 and TCP1 are key HCV-associated proteins in DEPs. The HCV group had 684 DEGs compared to the Ctrl group, and the chronic HCV group had 350 DEGs compared to the HCV group. DEGs primarily encode the extracellular matrix and regulate wound healing, cellular communication, oxidative stress, cell adhesion, viral infection, and immunity. KIF11, CENPE, TTK, CDC20 and ASPM are HCV-related hub genes in DEGs. Combined analyses revealed interactions between DEPs and DEGs, especially EIF4A3, MNAT1, and UBE2D1. Moreover, the expression patterns of EIF4A3, EIF2B1, MNAT1, SNRNP70, and UBE2D1 in DEPs/DEGs from Ctrl, HCV, and chronic HCV groups were consistent with the sequencing results.

Conclusion EIF4A3, EIF2B1, MNAT1, SNRNP70, and UBE2D1 are involved in the process of HCV infection and pathogenesis, and they may be potential biomarkers for the treatment of patients with hepatitis C.

Keywords Hepatitis C, Hepatitis C virus, Proteomics, Transcriptomics

[†]Jianqiong Wang and Andong Xia contributed equally to this work.

*Correspondence:

Rui Tao
mychili@qq.com
Wei Yue
1205914543@qq.com

¹Department of Clinical Laboratory, The First People's Hospital of Yunnan Province, The Affiliated Hospital of Kunming University of Science and Technology, No.157 Jinbi Road, Kunming, Yunnan, China

²Department of Infectious Diseases and Liver Diseases, The First People's Hospital of Yunnan Province, The Affiliated Hospital of Kunming University of Science and Technology, No.157 Jinbi Road, Kunming, Yunnan, China



© The Author(s) 2025. **Open Access** This article is licensed under a Creative Commons Attribution-NonCommercial-NoDerivatives 4.0 International License, which permits any non-commercial use, sharing, distribution and reproduction in any medium or format, as long as you give appropriate credit to the original author(s) and the source, provide a link to the Creative Commons licence, and indicate if you modified the licensed material. You do not have permission under this licence to share adapted material derived from this article or parts of it. The images or other third party material in this article are included in the article's Creative Commons licence, unless indicated otherwise in a credit line to the material. If material is not included in the article's Creative Commons licence and your intended use is not permitted by statutory regulation or exceeds the permitted use, you will need to obtain permission directly from the copyright holder. To view a copy of this licence, visit <http://creativecommons.org/licenses/by-nc-nd/4.0/>.

Introduction

Hepatitis C is an infectious liver damage disease caused by hepatitis c virus (HCV) infection and is one of the major causative factors of chronic severe liver disease. According to the World Health Organization, more than 325 million people worldwide are infected with different types of hepatitis viruses, with more than 50 million people chronically infected with HCV, and growing by 1 million new cases each year [1]. About 16% of patients with hepatitis C progress to cirrhosis after 20–30 years, and once cirrhosis occurs, about 1.4–4.9% progress to hepatocellular carcinoma (HCC) [2, 3]. The standard approach for HCV infection is polyethylene glycol-interferon α combined with ribavirin, which is effective in 70–80% of patients with HCV genotypes 2/3 and in 45–60% of patients with genotypes 1/4 [4–6]. However, this therapeutic strategy can cause a variety of adverse effects, including flu-like symptoms, blood cell changes, depression and autoimmune disorders [6–8]. Although, there are novel direct-acting antiviral agents (DAAs) that are more effective and have fewer side effects. This approach may lead to the development and recurrence of HCC [9–11]. Therefore, there is still a need for continued research into the mechanisms of HCV infection and pathogenesis.

Transcriptomics is a genome-wide measure of mRNA expression levels based on DNA microarray technology [12]. Proteomics is a method for tracking and comparing genome-wide gene expression at the protein level [13]. Transcriptomics and proteomics provide systematic assays and analyses at the mRNA and protein levels to reveal the molecular mechanisms of complex biological pathways and regulatory networks. The molecular mechanisms of HCV infection and pathogenesis have been revealed by transcriptomics and proteomics. Sabrina et al. [14] found that antibodies and T cells act synergistically in clearing HCV reinfection, and Valeria et al. [15] revealed molecular features associated with HCV-induced hepatocellular carcinoma through transcriptomics. Transcriptomics revealed that miR-122 promotes RNA replication by targeting two loci in the HCV genome [16]. In the HCV-related clinical trial, the miR-122 inhibitor Miravirsin is an effective therapeutic strategy with no long-term safety concerns [17, 18]. Moreover, proteomics revealed that the interaction of nucleoporin Nup98 with capsid proteins is required for HCV morphogenesis [19], and that AFP, UGT1, and HCV NS4B are novel molecular chaperones for HCV envelop protein E2 [20]. The proteomic discovery of the interaction of the viral protein NS5A with host proteins laid the foundation for the development of NS5A inhibitors, which have been successfully used in the treatment of DAAs [21, 22]. Notably, transcriptomics or proteomics data alone provide only partial information on transcription or translation. The combined analysis of transcriptomics

and proteomics allows for a more comprehensive and in-depth understanding of the entire life activities of an organism [23, 24].

In conclusion, the present study intends to comprehensively analyze and compare the serum molecular profiles of normal population, population with previous HCV infection and patients with persistent HCV hepatitis C infection through transcriptomics and proteomics. The aim is to provide molecular mechanisms and potential biomarkers related to HCV infection and pathogenesis for the treatment of hepatitis C.

Materials and methods

Clinical samples

Serum samples for this study were collected from the First People's Hospital of Yunnan Province. The Ethics Committee of the First People's Hospital of Yunnan Province and the subjects approved this study (Approval No. 2020KYS112), and the subjects signed an informed consent form. The groups of serum samples were set up as Ctrl, HCV and chronic HCV, with 4 cases in each group. The Ctrl group was phenotyped as HCV Ab⁻ and HCV RNA⁻, indicating the absence of HCV infection. The HCV group was defined as HCV Ab⁺ and HCV RNA⁻, indicating a past infection without current viral presence. The chronic HCV group is characterized by HCV Ab⁺ and HCV RNA⁺, signifying a persistent infection. Patients with hepatitis C were diagnosed in accordance with Guidelines for the prevention and treatment of hepatitis C (2019 version) [25] and the prevention and treatment of hepatitis C (2022 version) in China [26]. Patients with hepatitis C meet the criteria of HCV infection for more than 6 months and liver histopathology consistent with chronic hepatitis. Patients with a history of previous thyroid disease, comorbidities with other viral hepatitis and other chronic liver diseases (Cirrhosis, HCC, Alcoholic liver disease, and Fatty liver disease), those presenting with periods of hepatic decompensation, and those who were pregnant and breastfeeding were excluded.

Proteomics analysis

Proteome expression profiles of serum samples from Ctrl, HCV and chronic HCV groups identified using TMT. TMT was performed with OEBioTech (Shanghai, China; DZLM2023110240). Total protein extraction, concentration determination and SDS-PAGE electrophoretic analysis of serum samples from each group were accomplished by iTS kit (Omicsolution, China; P.O. 00027), BCA kit (Thermo Scientific, USA; 23225) and Tanon 1600 gel image analysis system (Tanon, China). Proteolysis, peptide labeling and desalting of protein samples were performed by 1 μ g/ μ L sequencing-grade trypsin (Coowins, China; HLS TRY001C), TMT (Thermo Scientific, USA; 90406), and desalting columns (Waters,

USA; WAT023590) with methanol and TFA. Proteomics analysis of all samples was done by Q-Exact mass spectrometer (Thermo, USA) and Nanospray Flex source (Thermo, USA). Briefly, protein samples were loaded and separated by C18 column and EASY-nLCTM 1200 system (Thermo, USA). Mobile phases A and B consisted of 0.1% FA in water and 0.1% FA in CAN. Flow rates and run times were 300 nL/min and 75 min. The scanning range, mass resolution and AGC target value of the mass spectra were 300~1600 m/z, 70,000 and 1×10^6 . The resolution, AGC target value and max injection time of the obtained MS/MS spectra were 17,500, 2×10^5 , and 80 ms. Q-E dynamic exclusion and run mode are 30 s and positive mode. The spectra of each run were retrieved and quantitatively analyzed using Spectronaut Pulsar 18.4 (Biognosys, Switzerland) software based on the uniprot-Homo sapiens-9606-2023.2.1.fasta database. Differential expression analysis and enrichment analysis were done by DESeq2 V. 1.22.2 [27] and the hypergeometric distribution algorithm and gene set enrichment analysis (GSEA) [28] based on GO [29] and KEGG [30] databases.

Transcriptomics analysis

RNA-seq was used to identify transcriptome expression profiles of serum samples from Ctrl, HCV and chronic HCV groups, and performed by OEBioTech (Shanghai, China; DZOE2023110197). Total RNA extraction, concentration determination, integrity assessment and transcriptome library construction for each group of serum samples were accomplished by TRIzol kit (Thermo Scientific, USA), NanoDrop 2000 spectrophotometer (Thermo Scientific, USA), Agilent 2100 Bioanalyzer (Agilent, USA) and VAHTS Universal V5 RNA-seq Library Prep kit (Vazyme, China). The sequencing platform was Illumina Novaseq™ 6000, generating 150 bp double-ended reads (PE150). RNA quality control, quality control of sequencing data, reference genome comparison, quantitative analysis, differential expression analysis and enrichment analysis were performed by RseqQC V.4.0.0 [31], fastp V.0.20.1 [32], hisat2 V.2.1.0 [33], HTSeq-count V.0.11.2 [34], DESeq2 V.1.22.2 [27], and the hypergeometric distribution algorithm and gene set enrichment analysis (GSEA) [28] based on the GO [29] and KEGG [30]. A total of 87.1 G raw bases were obtained from all the samples, ranging from 6.04 G to 7.64 G. After the quality control of raw bases, a total of 80.34 G clean bases were obtained for all samples, ranging from 5.59 G to 7.03 G. The mean of Q20 is 93.58% with a range of 93.39–93.79%. The mean of GC content for all samples was 49.99% with a range of 47.88–52.28%.

RT-qPCR assay

Total RNA was extracted from serum using TRIzol kit (Sangon, China; B511311-0500), and the optical density

value of total RNA at 260 nm was measured using a TGen Plus full-wavelength spectrophotometer (TianGen, Germany; OSE-260-02) for concentration detection. Total RNA was taken to perform reverse transcription and PCR amplification using OneStep RT-PCR Kit (QiaGen, Germany; 210215). Thermal cycling conditions were reverse transcription at 50 °C for 30 min, initial PCR activation step at 95 °C for 15 min, and 30 cycles of denaturation with 1 min at 94 °C, annealing with 1 min at 55 °C and extension with 1 min at 72 °C. The internal reference for EIF4A3, EIF2B1, MNAT1, SNRNP70 and UBE2D1 was GAPDH and the expression of target genes was calculated using the $2^{-\Delta\Delta CT}$ method [35]. Primers for EIF4A3 are GGAGATGACCAACAAGTTC (F) and TTGATGCCTTCCAGAGTC (R); primers for EIF2B1 are AATACTCCGATTACTCCAA (F) and ATATTGTCCGCTCCATCTT (R); primers for MNAT1 are GAAGTGGAACGACAGGAA (F) and GTGAATAGGTGCCAGTGA (R); primers for SNRNP70 are ATTATGACACAACA GAATCCAA (F) and TGACCGCTTACTGTAGAC (R); primers for UBE2D1 were CGATATTCTGAGGTCACA (F) and GGTCATCTGGGATTAGGAT (R); primers for GAPDH are TTGCCCTCAACGACCACTTT (F) and TGGTCCAGGGGTCTTACTCC (R).

Western blot assay

Total serum proteins were extracted using RIPA protein lysate (Proteintech, USA; PR20035) and the optical density values of total serum proteins at 280 nm were determined using a TGen Plus full-wavelength spectrophotometer (TianGen, Germany; OSE-260-02) for concentration detection. After 12% SDS-PAGE electrophoresis, the membrane was transferred to a PVDF membrane using a Trans-Blot (Bio-Rad, USA; 1703850). After blocking, PVDF membranes were supplemented with anti-EIF4A3 (Abcam, USA; ab180573; 1:2000), anti-EIF2B1 (Abcam, USA; ab181186; 1:10000), anti-MNAT1 (Proteintech, USA; 11719-1-AP; 1:50000), anti-SNRNP70 (Abcam, USA; ab83306; 1:1000), anti-UBE2D1 (Abcam, USA; ab176561; 1:50000), anti- β -actin (ZSGB-Bio, China; TA-09; 1:4000), Goat Anti Mouse IgG-HRP (Abmart, China; M21001L; 1:4000), and Goat Anti Rabbit IgG-HRP (Abmart, China; M21002L; 1:4000) to incubate. PVDF membranes were exposed and images were collected in a GelDoc XR + Gel Imaging System (Bio-Rad, USA; 1708195), and gray-scale values were quantified using Image Lab software (Bio-Rad, USA; 1708195).

Statistical analysis

For proteomics, data were screened for differentially expressed proteins (DEPs) using apply combined with the sweep function to implement median normalization and log₂ transformation, and using DESeq2 V.1.22.2 [27] to perform negative binomial distribution tests.

For transcriptomics, the data were used to normalize the counts of genes and differential expression analysis using the DESeq2 R package to screen for differentially expressed genes (DEGs). DEPs and DEGs conformed to $|\log_2FC| > 1$ and $P < 0.05$. For expression verification, data from RT-qPCR and western blot assays were repeated four times and statistically analyzed using GraphPad Prism software (GraphPad, USA). One-way ANOVA with Tukey's multiple comparisons test was used for differential analysis of data. $P < 0.05$ represents a statistically significant difference.

Results

Identification of depts in the serum of patients with HCV

In serum proteomics, a total of 17,811 peptides and 2,084 proteins were identified in 12 samples (Fig. 1A), and 1,655, 1,496, and 1,544 proteins were present in chronic HCV, HCV, and Ctrl samples, respectively (Fig. 1B). After normalization of the protein expression profiles, the median value of protein expression abundance for all samples was essentially at one level and the data for each sample was relatively centralized (Fig. 1C). PCA analysis revealed that the protein profiles of chronic HCV, HCV and Ctrl group were unsupervised aggregation within groups and discrete between groups (Fig. 1D). This suggests that the protein profiles of the three groups differed considerably in overall. Differential expression analysis revealed that compared to the Ctrl group, the HCV group had 356 DEPs in serum, including 220 significantly down-regulated and 136 significantly up-regulated DEPs; compared to the HCV group, the chronic HCV group had 133 significantly down-regulated and 248 significantly up-regulated DEPs in serum, for a total of 381 DEPs (Fig. 1E and Supplementary file S1). Moreover, the protein profiles of samples from the same group exhibited clustering and those between different groups were discrete, and the DEPs of samples from different groups had unique expression profiles (Fig. 1F). This further validates the results of PCA. Venn demonstrated the presence of 597 concatenating DEPs and 140 intersecting DEPs in HCV-vs-Ctrl and chronic HCV-vs-HCV (Fig. 1G).

Enrichment analysis of depts in the serum of patients with HCV

In this study, we identified the possible biological functions and related molecular mechanisms regulated by DEPs using enrichment analysis. As shown in Fig. 2A and C, DEPs in HCV-vs-Ctrl are mainly immunoglobulins, exosomal proteins, and cellular matrix proteins, which may regulate carbon dioxide transport, initiation of transcription, immune response, organic acid metabolism, platelet activation, bacterial and viral infection, and glutathione metabolism (Supplementary file S2). In addition,

DEPs in chronic HCV-vs-HCV DEPs are mainly cytoskeletal, exosomal and cytosolic matrix proteins that may regulate cytoskeleton, cytoplasmic translation, muscle contraction, cell adhesion, bacterial and viral infections, glucose metabolism, platelet activation, extracellular matrix (ECM), and endocytosis (Fig. 2B and D; Supplementary file S2).

Further, this study identified the role of DEPs in the regulation of GO term and KEGG pathway using GSEA. As indicated in Fig. 3A-3B, DEPs in HCV-vs-Ctrl facilitate "regulation of inflammatory response", "response to endoplasmic reticulum stress", "sphingolipid signaling pathway", and "adherens signaling pathway", and inhibited "peptide cross-linking", "cholesterol metabolic process", "NF-kappa B signaling pathway" and "intestinal immune network for IgA production" (Supplementary file S3). DEPs in chronic HCV-vs-HCV contribute to "positive regulation of GTPase activity", "transmembrane transporter binding", "hypertrophic cardiomyopathy" and "fluid shear stress and cardiovascular disease", and suppressed "cytosolic small ribosomal subunit", "translational initiation", mRNA surveillance pathway" and "Ribosome" (Fig. 3A-3B; Supplementary file S3).

PPI network of depts in the serum of patients with HCV

In this study, key proteins of DEPs were analyzed by String database and Cytoscape software. The PPI network of DEPs in HCV-vs-Ctrl has 328 nodes and 5,598 relationship pairs (Supplementary file S4). The PPI network of the DEPs with Degree TOP25 is shown in Fig. 4A, and the PPI network contains 250 relationship pairs. HSPA4, HSPD1, COPS5, PSMD2 and TCP1 are Degree TOP5 in this PPI network, and they were significantly under-expressed in the serum of the HCV group (Fig. 4A). In chronic HCV-vs-HCV, the PPI network associated with DEPs contains 364 nodes and 7,413 edges (Supplementary file S4). In addition, the PPI network of the DEPs with Degree TOP25 contains 222 edges (Fig. 4B). In this PPI network, ACTB, PSMD14, YWHAZ, CCT2 and ACTR3 were Degree TOP5, and ACTB, YWHAZ, CCT2 and ACTR3 were hyper-expressed in the serum of the chronic HCV group, and PSMD14 was vice versa (Fig. 4B). This study further identified the key sub-networks of the PPI network using the MCODE algorithm. In the HCV-vs-Con, the clustering scores of the top 3 subnetworks were 9.33, 5, and 3.5, and the number of nodes were 10, 5, and 5, respectively (Fig. 4C). These hub DEPs primarily regulate mRNA metabolic processes, oxidative stress, oxygen transport, and virus-associated diseases (Supplementary Fig. S1A and Supplementary file S9). In the chronic HCV-vs-HCV, the clustering scores of the top 3 sub-networks were 13.875, 6, and 5.6, with the number of nodes being 17, 6, and 6, respectively (Fig. 4D). These hub DEPs primarily modulate translation, Cajal

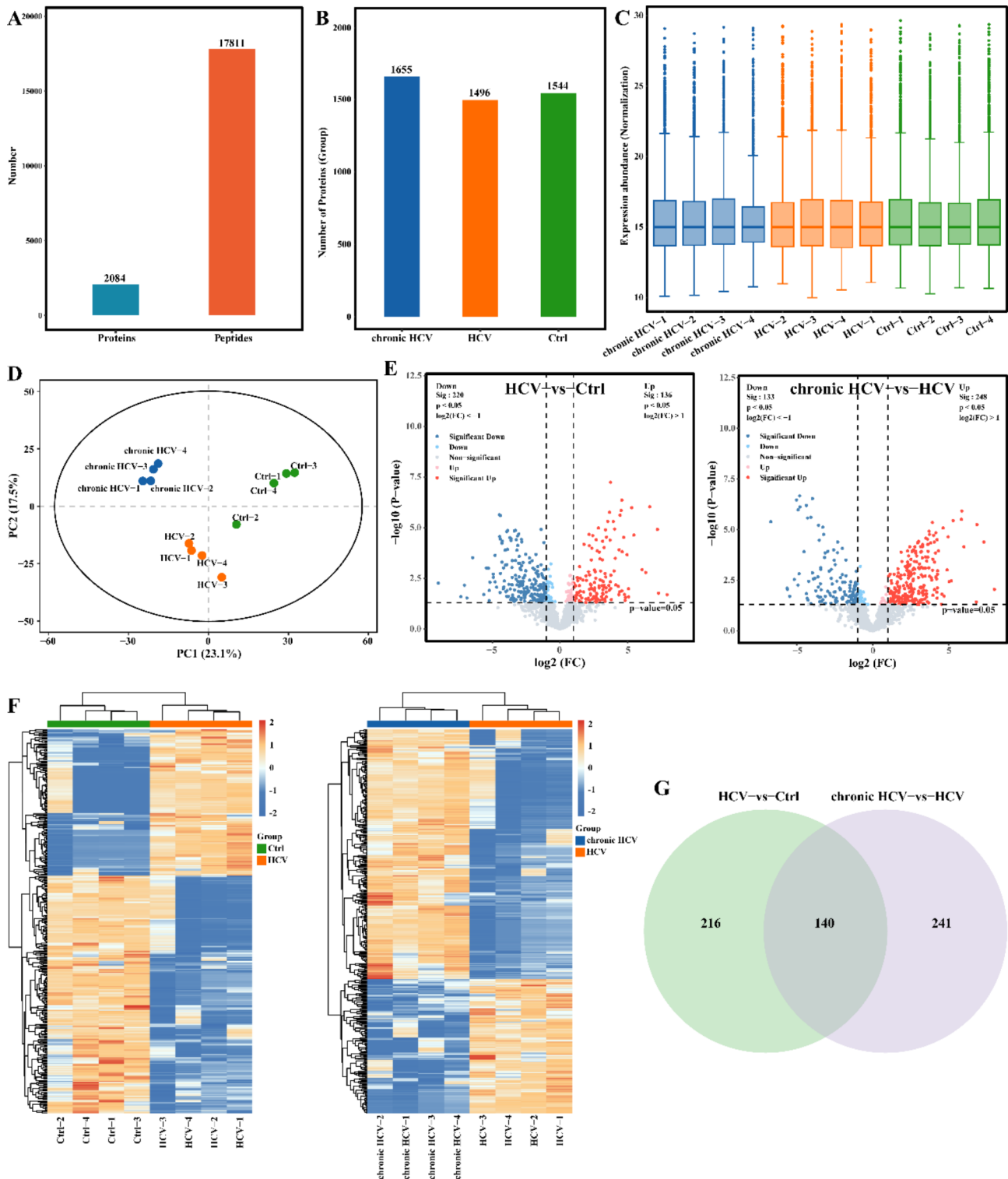


Fig. 1 Identification of HCV-associated differentially expressed proteins (DEPs). **A:** Bar graph shows the number of proteins and peptides identified in twelve samples. **B:** Number of proteins with chronic HCV, HCV and Ctrl group serum samples. **C:** Expression abundance and distribution of all proteins in the chronic HCV, HCV and Ctrl groups after data calibration. **D:** Principal Component Analysis (PCA) was used to analyze the protein expression profiles of serum samples from the chronic HCV, HCV, and Ctrl groups to take an overall view of the differences between and within groups for each sample. **E:** Volcano plots visualize the number and distribution of DEPs in HCV+vs-Ctrl (left) and chronic HCV+vs-HCV (right). DEP satisfies $|\log_2(FC)| > 1$ and $P < 0.05$. **F:** Heatmaps exhibit clustering results of samples and expression profiles of DEPs in HCV+vs-Ctrl (left) and chronic HCV+vs-HCV (right). **G:** Venn diagram visualizes the number of intersecting and concatenating DEPs in HCV+vs-Ctrl and chronic HCV+vs-HCV

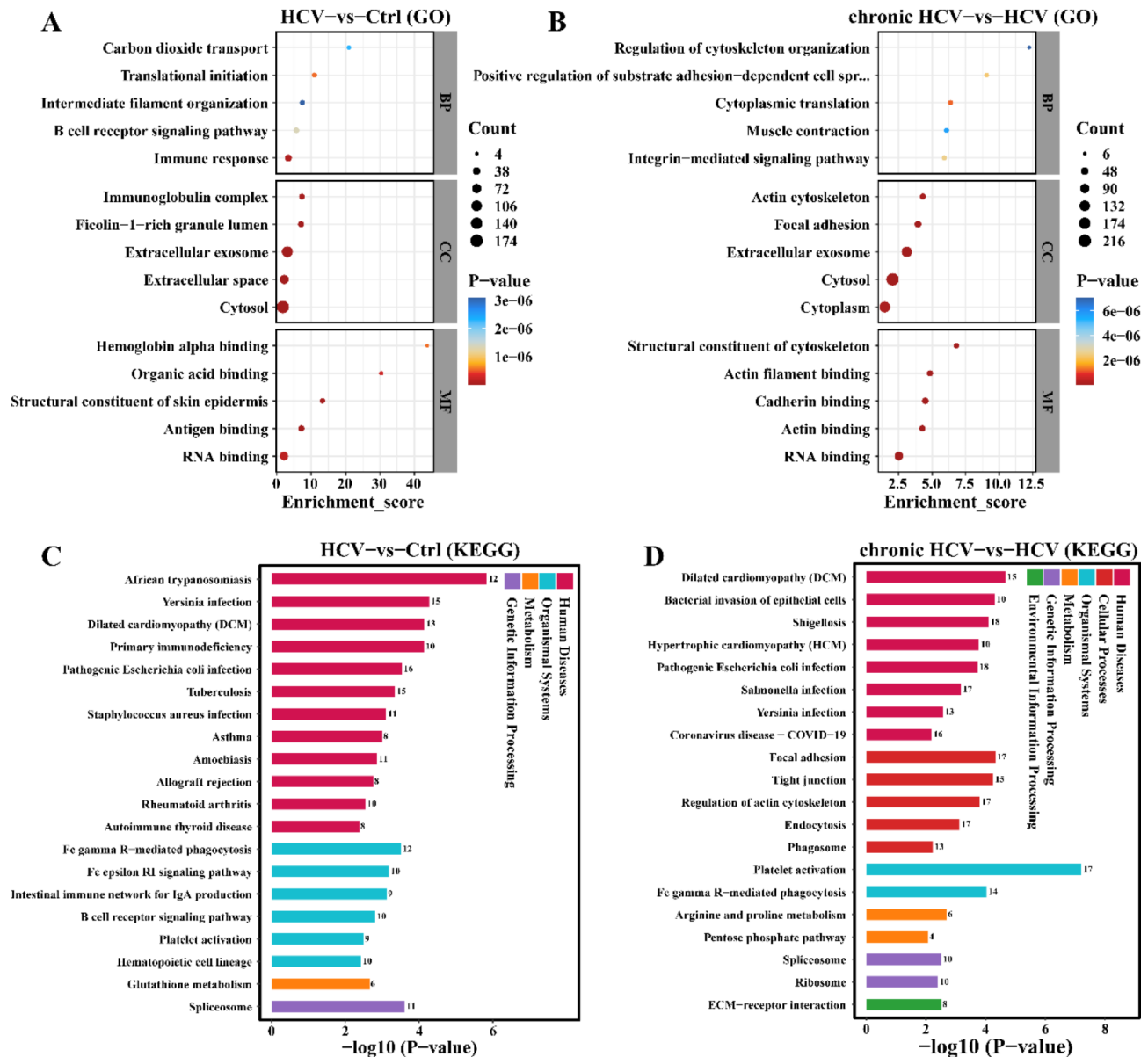


Fig. 2 GO and KEGG enrichment analysis of HCV-associated DEPs. **A-B:** GO enrichment analysis results of DEPs in HCV-vs-Ctrl (**A**) and chronic HCV-vs-HCV (**B**). Bubble diagrams display the five GO terms with the smallest p-value in Biological Processes (BP), Cell Composition (CC) and Molecular Function (MF). **C-D:** KEGG enrichment analysis results of DEPs in HCV-vs-Ctrl (**C**) and chronic HCV-vs-HCV (**D**). Bar graphs demonstrate the twenty KEGG pathways with the smallest p-value in KEGG Level 3

bodies, cytoskeleton, and bacterial and viral infection (Supplementary Fig. S1B and Supplementary file S9).

Identification of DEGs in the serum of patients with HCV

This study identified the transcriptome expression profiles of serum samples from the chronic HCV, HCV, and Ctrl groups, and characterized the DEGs. As indicated in Fig. 5A, the median values of FPKM data of serum samples from chronic HCV, HCV and Ctrl groups were essentially the same and symmetrical after normalization of sequencing data. The transcriptome expression profiles of the HCV and Ctrl groups had large distances,

and chronic HCV was closer to the HCV and Ctrl groups (Fig. 5B). DESeq2 package analysis demonstrated that compared to the Ctrl group, the HCV group had 684 DEGs, including 238 significantly down-regulated and 446 significantly up-regulated DEGs (Fig. 5C and Supplementary file S5); compared to the HCV group, there were 202 significantly down-regulated and 148 significantly up-regulated DEGs in the chronic HCV group, totaling 350 DEGs (Fig. 5F and Supplementary file S5). Heatmaps displayed that DEGs from different groups had different expression patterns and clustered within groups and discrete between groups (Fig. 5D and G). In HCV-vs-Ctrl,

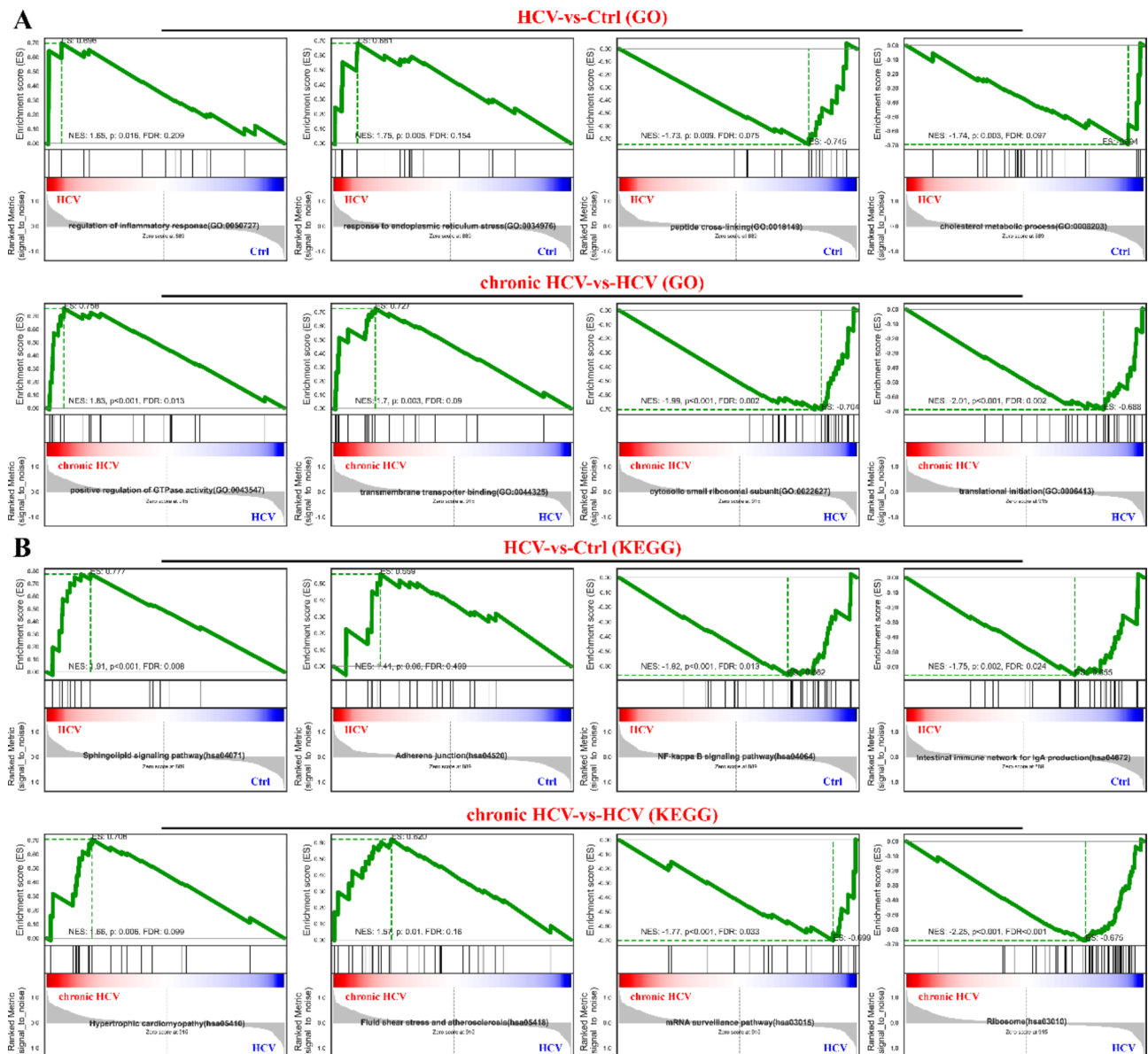


Fig. 3 Gene set enrichment analysis (GSEA) of HCV-associated DEPs. **A:** GSEA for GO enrichment analysis results in HCV-vs-Ctrl (top) and chronic HCV-vs-HCV (bottom). GSEA plots show the GO term with|ES| TOP4. **B:** GSEA for KEGG enrichment analysis results in HCV-vs-Ctrl (top) and chronic HCV-vs-HCV (bottom). GSEA plots show the KEGG pathway with|ES| TOP4

DEGs with $|\log_2FC|$ TOP5 were USP9Y, ZFY, RPS4Y1, KDM5D, and UTY, and they were significantly over-expressed in the serum of the HCV group (Fig. 5E). In chronic HCV-vs-HCV, LOC105377884, LOC105377885, LOC107985235, GRIK4, and C4BPA were the DEGs with $|\log_2FC|$ TOP5, and GRIK4 was significantly hyper-expressed in the serum of the chronic HCV group, and the others were vice versa (Fig. 5H). Notably, the number of intersecting and concatenating DEGs in HCV-vs-Ctrl and chronic HCV-vs-HCV were 122 and 912, respectively (Fig. 5I).

Enrichment analysis of DEGs in the serum of patients with HCV

In HCV-vs-Ctrl, DEGs primarily encode ECM and hemoglobin, which regulate wound healing, cellular communication, blood coagulation, carbon dioxide and oxygen transport, organic acid metabolism, oxidative stress, cellular adhesion, ECM and receptor interactions, viral infection, and immunity, in association with the Hippo, Apelin, cAMP and PI3K-Akt pathways (Fig. 6A and C; Supplementary file S6). In chronic HCV-vs-HCV, DEGs mainly encode AP-2 adaptor and ECM, which regulate cell cycle, amino acid metabolism, complement system, nitrogen metabolism, cell adhesion, cytoskeleton,

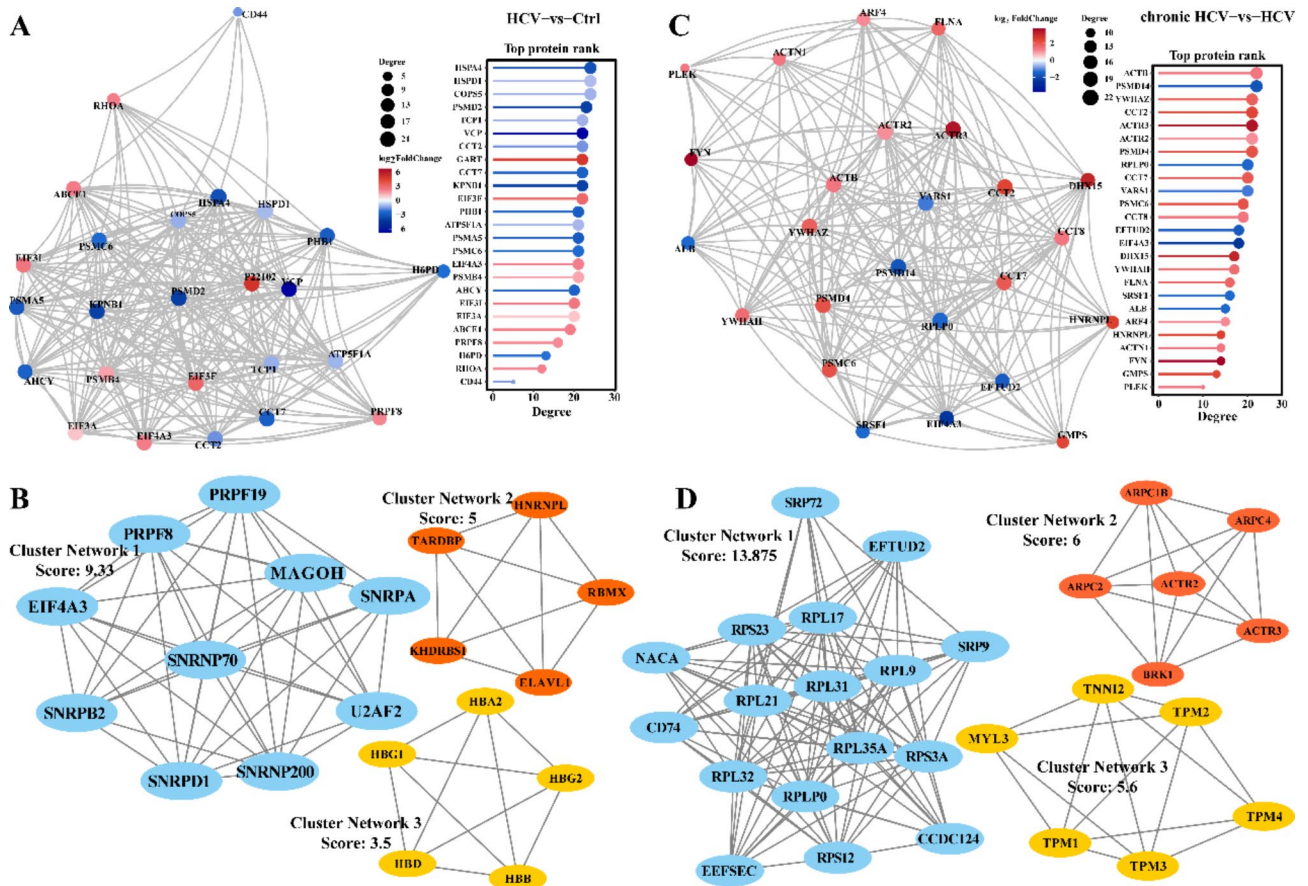


Fig. 4 Protein-protein interaction (PPI) network of HCV-associated DEPs. **A-B:** PPI network of DEPs with Degree TOP30 in HCV-vs-Ctrl (**A**) and chronic HCV-vs-HCV (**B**) as well as top protein rank of each node. The size and color of the nodes represent degree and \log_2FC , respectively. Larger nodes or darker colors represent larger degrees or $|\log_2FC|$; red or blue nodes represent up-regulation or down-regulation. **C-D:** The MCODE algorithm was used to identify key sub-networks of DEPs-related PPI networks in HCV-vs-Ctrl (**C**) and chronic HCV-vs-HCV (**D**)

immunity, cytokine interactions, hematopoiesis, and nucleotide metabolism, and the Rap1 and PI3K-Akt pathways (Fig. 6B and D; Supplementary file S6). GSEA results revealed that, in HCV-vs-Ctrl, DEGs favored “fibrinolysis”, “long-chain fatty-acyl-CoA biosynthetic process”, “nicotine addiction” and “staphylococcus aureus infection, and inhibited “small ribosomal subunit”, “RNA export from nucleus”, “other glycan degradation” and “Arginine biosynthesis” (Fig. 7A-7B; Supplementary file S7). In chronic HCV-vs-HCV, DEGs facilitate “L-glutamate transmembrane transport”, “response to vitamin A”, “starch and sucrose metabolism” and “RNA polymerase”, and inhibited the “regulation of postsynaptic membrane potential”, “positive regulation of dendritic spine morphogenesis”, “vasopressin-regulated water reabsorption” and “one carbon pool by folate” (Fig. 7A-7B; Supplementary file S7).

PPI network of DEGs in the serum of patients with HCV

In HCV-vs-Ctrl, the DEGs-associated PPI network has 455 genes and 5,386 interaction pairs (Supplementary

file S8). In chronic HCV-vs-HCV, the DEGs associated PPI network has 228 nodes and 1,168 edges (Supplementary file S8). The PPI network of DEGs with interaction TOP30 in HCV-vs-Ctrl is shown in Fig. 8A. The network contains 25 nodes and the Degree TOP5 are KIF11, CENPE, TTK, CDC20 and ASPM, which are all significantly over-expressed in the serum of the HCV group (Fig. 8A). In chronic HCV-vs-HCV, the PPI network of DEGs with interaction TOP30 contained 38 genes (Fig. 7B). Notably, the Degree TOP5 in this network were C3, ORM2, PTGFR, IGF1, and C4B (Fig. 8B). ORM2, PTGFR, and IGF1 were significantly expressed in the serum of the chronic HCV group, and the reverse was true for C3 and C4B (Fig. 8B). MCODE analysis revealed that, in the HCV-vs-Con, the clustering scores of the top 3 ranked sub-networks were 13.429, 9.778, and 4.5, with the number of nodes being 17, 10, and 5, respectively (Fig. 8C). These hub DEGs primarily regulate the cell cycle, fibrinolysis, cytoskeleton, and bacterial and viral infection, as well as the Rap1, HIF-1, EGFR, and p53 pathways (Supplementary Fig. S2A and Supplementary

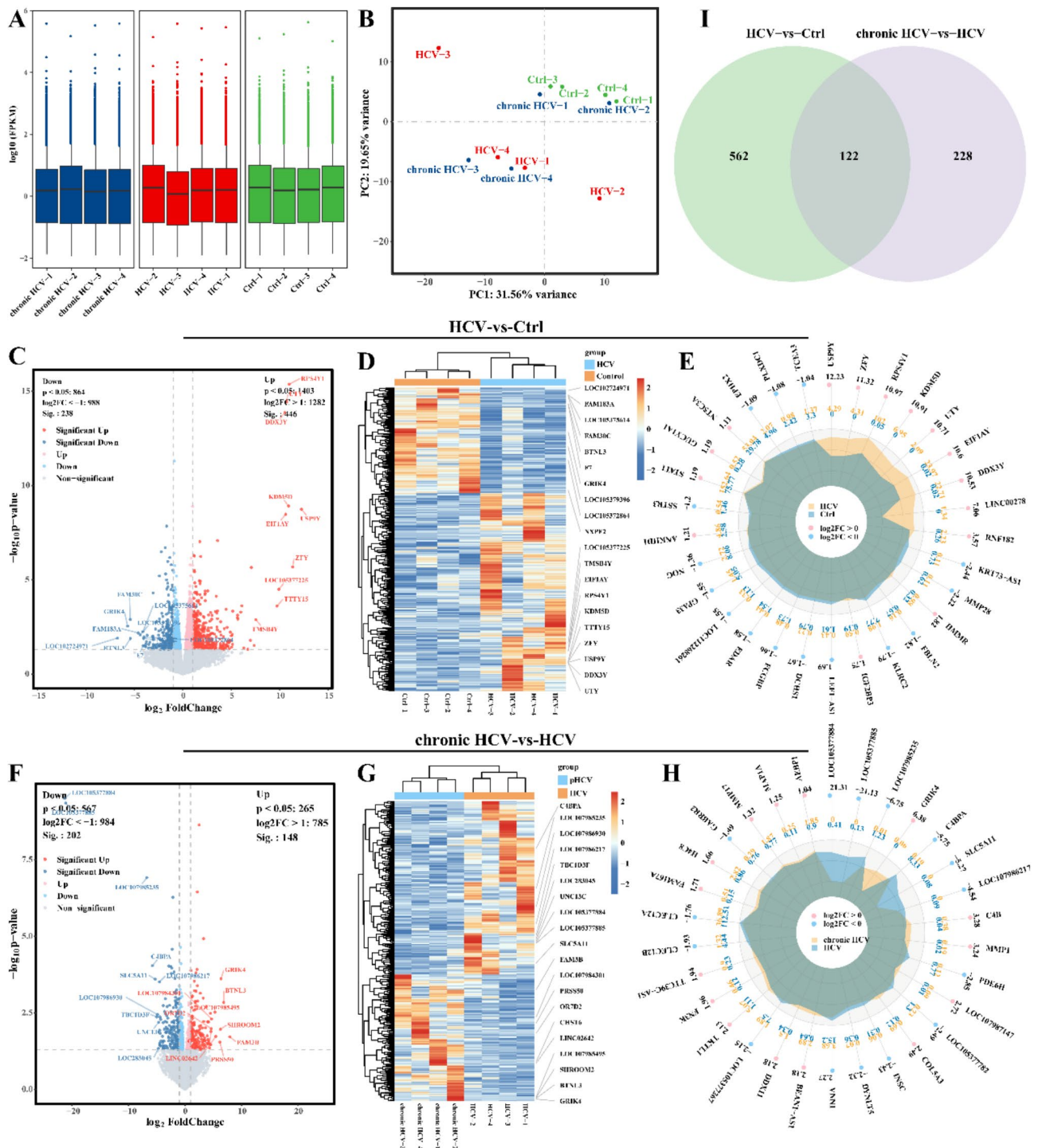


Fig. 5 Identification of HCV-associated differentially expressed genes (DEGs). **A:** $\log_{10}(\text{FPKM})$ and distribution of all genes in the chronic HCV, HCV and Ctrl groups after data calibration. **B:** The mRNA expression profiles of serum samples from the chronic HCV, HCV and Ctrl groups were dimensionalized with PCA for an overall view of the differences between and within groups for each sample. **C** and **F:** Volcano plots visualize the number and distribution of DEPs in HCV-vs-Ctrl (**C**) and chronic HCV-vs-HCV (**F**). DEG satisfies $|\log_2\text{FC}| > 1$ and $P < 0.05$. **D** and **G:** Heatmaps display clustering results of samples and DEG expression profiles in HCV-vs-Ctrl (**D**) and chronic HCV-vs-HCV (**G**). **E** and **H:** Radar plots exhibit the TOP30 DEGs and their corresponding $\log_2\text{FC}$ in HCV-vs-Ctrl (**E**) and chronic HCV-vs-HCV (**H**). **I:** Venn diagram visualizes the number of intersections and concatenations of DEGs in HCV-vs-Ctrl and chronic HCV-vs-HCV

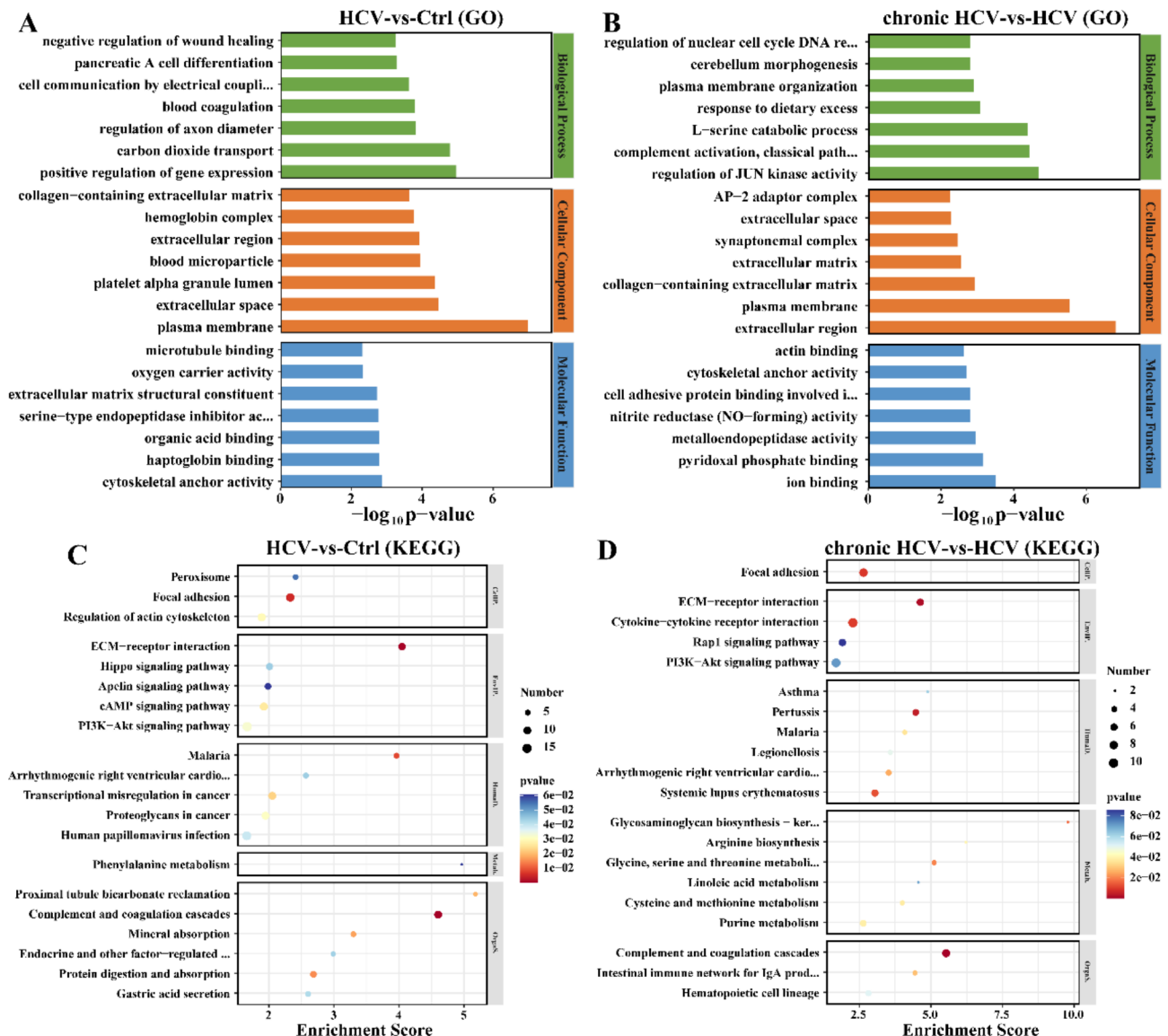


Fig. 6 GO and KEGG enrichment analysis of HCV-associated DEGs. **A-B:** Results of GO enrichment analysis for DEGs in HCV-vs-Ctrl (**A**) and chronic HCV-vs-HCV (**B**). Bar graphs show the 7 GO terms with the smallest p-value in BP, CC and MF. **C-D:** Results of GO enrichment analysis for DEGs in HCV-vs-Ctrl (**C**) and chronic HCV-vs-HCV (**D**). Bubble diagrams illustrate the 20 KEGG pathways with the smallest p-value in KEGG Level 3

file S10). In the chronic HCV-vs-HCV, the top 2 sub-networks have clustering scores of 3.333 and 3, and the number of nodes of 4 and 3, respectively (Fig. 8D). These hub DEGs primarily modulate immune response, complement system, extracellular matrix, and bacterial and viral infections, as well as PI3K-Akt pathway (Supplementary Fig. S2B and Supplementary file S10).

Combined analysis of proteomics and transcriptomics of serum from patients with HCV

In this study, the interactions between HCV-associated DEPs and DEGs were identified using OmicsNet and InnateDB database. The data analyzed were intersections in HCV-vs-Ctrl and chronic HCV-vs-HCV with

140 DEPs and 122 DEGs. As shown in Fig. 9A, the OmicsNet analysis obtained a total of 11 networks. The largest network contains 11 nodes and 10 relation pairs with 10 DEPs and 1 DEGs, and EIF4A3 is the node with the largest degree (Fig. 8A). The second largest network contains 10 nodes and 9 relation pairs with 5 DEPs and 5 DEGs, and MNAT1 and UBE2D1 are the nodes with the largest degree (Fig. 8A). In addition, FRK interacts with CSK and KHDRBS1, FHIT with ETVB and ALDH2, and SIK1 with PRKACA (Fig. 8A). In this study, EIF4A3, EIF2B1, MNAT1, SNRNP70 and UBE2D1 were selected for validation in serum samples. Compared to the Ctrl group, the expression of EIF4A3, EIF2B1, SNRNP70 and UBE2D1 mRNA was significantly increased and

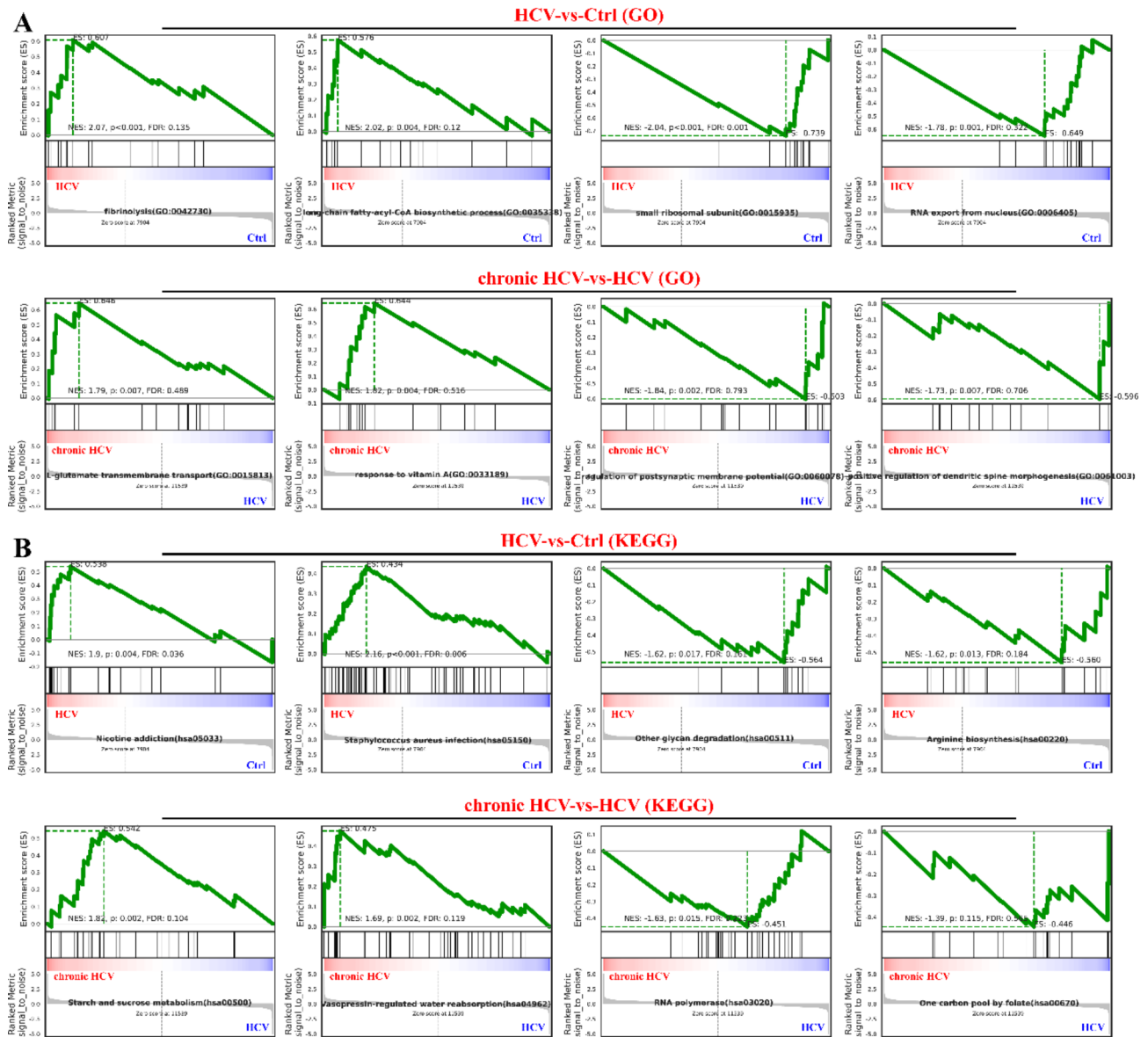


Fig. 7 GSEA analysis of HCV-associated DEGs. **A:** GSEA analysis for GO enrichment results in HCV-vs-Ctrl (top) and chronic HCV-vs-HCV (bottom). The GSEA plots show the GO term for the|ES| Top 4. **B:** GSEA analysis for KEGG enrichment results in HCV-vs-Ctrl (top) and chronic HCV-vs-HCV (bottom). The GSEA plots show the KEGG pathway for the|ES| Top 4

the expression of MNAT1 was significantly decreased in the HCV group (Fig. 9B). Compared with the HCV group, the expression of EIF4A3, EIF2B1, SNRNP70 and UBE2D1 mRNA was significantly decreased and the expression of MNAT1 was significantly increased in the chronic HCV group (Fig. 9B). Moreover, protein expression of EIF4A3, EIF2B1, MNAT1, SNRNP70, and UBE2D1 showed a similar pattern (Fig. 9C). This result is consistent with the sequencing results (Supplementary file S1 and Supplementary file S5).

Discussion

In this study, we analyzed and compared the serum molecular profiles of normal population (Ctrl group), population with previous HCV infection (HCV group), and patients with persistent HCV infection (chronic HCV group) using a combination of transcriptomics and proteomics. Compared to the Ctrl group, the HCV group had 356 DEPs and 684 DEGs in serum; compared to the HCV group, the chronic HCV group had 381 DEPs and 350 DEGs in serum. In enrichment analyses, DEPs/DEGs predominantly regulated cellular communication, wound healing, oxidative stress, cell adhesion, viral infection, and immunity, and were associated with the Rap1,

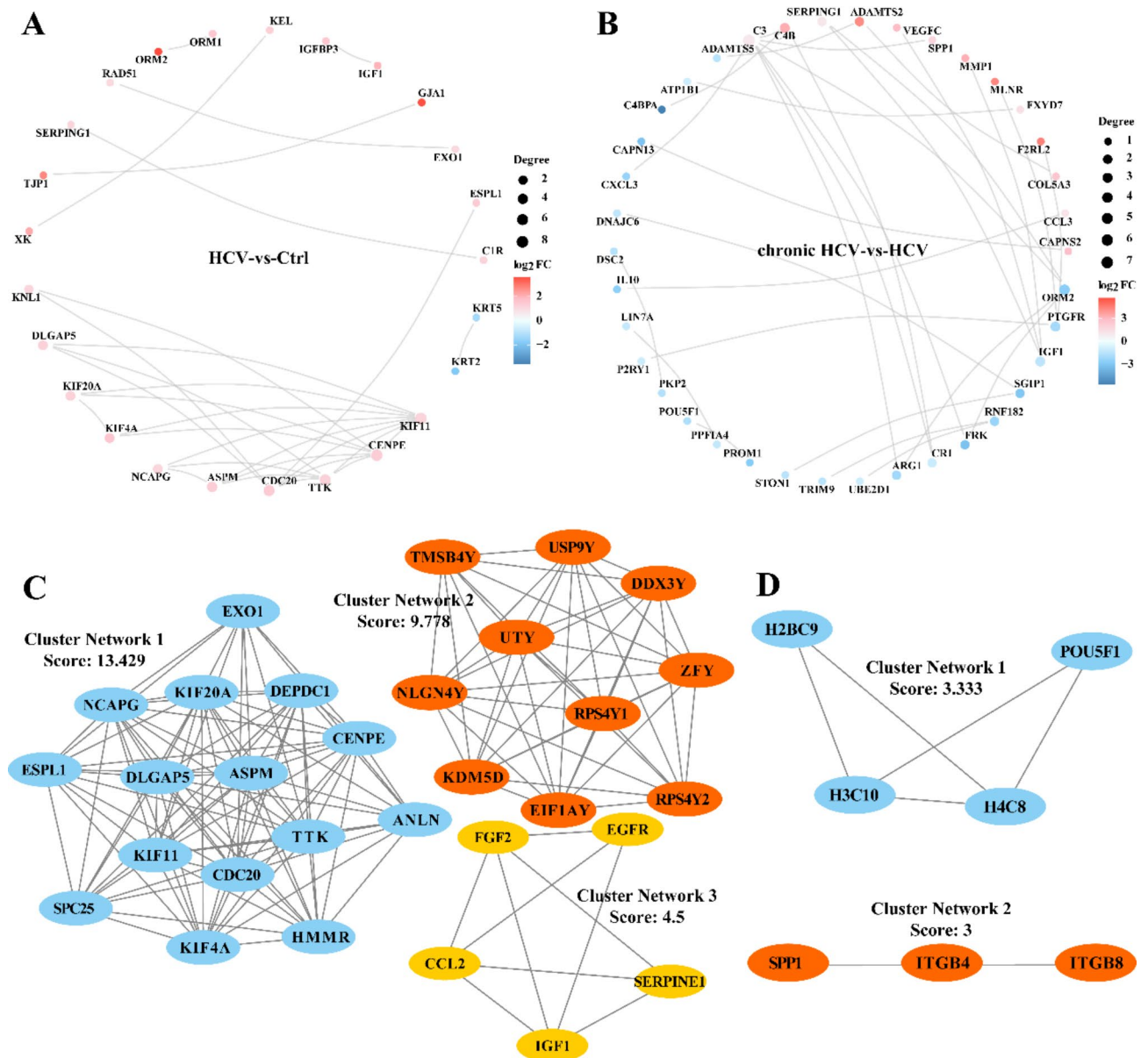


Fig. 8 PPI network of HCV-associated DEGs. **A-B:** PPI network of DEGs with Degree TOP30 in HCV-vs-Ctrl (**A**) and chronic HCV-vs-HCV (**B**). The size and color of the nodes represent degree and \log_2FC , respectively. Larger nodes or darker colors represent larger degrees or $|\log_2FC|$; red or blue nodes represent up-regulation or down-regulation. **C-D:** The MCODE algorithm was used to identify key sub-networks of DEGs-related PPI networks in HCV-vs-Ctrl (**C**) and chronic HCV-vs-HCV (**D**)

Hippo, cAMP, and PI3K-Akt pathways. Notably, these pathways have been demonstrated to regulate HCV-associated disease processes and liver injury phenotypes [36–38]. Moreover, HSPA4, HSPD1, COPS5, PSMD2, TCP1, KIF11, CENPE, TTK, CDC20, and ASPM are key hubs in DEPs/DEGs. Interestingly, some key hubs have been identified to regulate HCV infection and pathogenesis.

HSPA4, a member of the heat shock protein family A (Hsp70), plays a crucial role in maintaining the cell cycle, protein homeostasis and response to environmental stresses [39]. Notably, Hsp70 promotes viral

replication, assembly, and release by interacting with key factors (NS5A, lipid droplet-associated proteins, HCV core proteins) at various stages of the HCV life cycle and is an important host factor in HCV infection [40]. Currently, an inhibitor of Hsp70 (VER-155008) is undergoing preclinical trials and it has been demonstrated that VER-155,008 can effectively inhibit HCV assembly [41]. HSPA4 expression was increased in serum of patients with HCV-associated cirrhosis, early HCC, and advanced HCC in a stepwise manner, and the level of HSPA4 could distinguish HCV-associated cirrhosis from HCC [42].

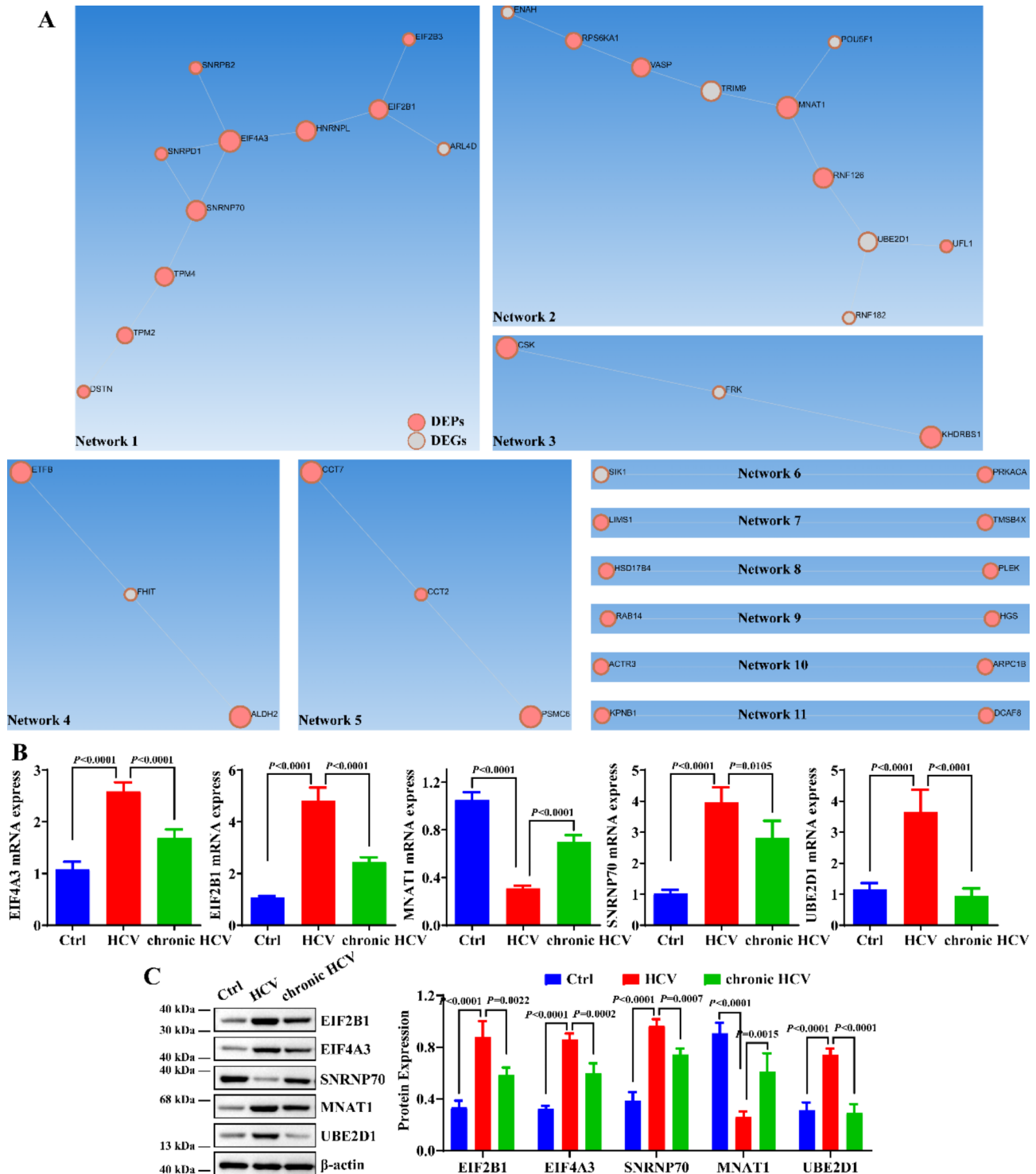


Fig. 9 Combined analysis of proteomics and transcriptomics of serum from patients with HCV. **A:** OmicsNet recognizes interactions between DEPs and DEGs. Red or gray color represents DEPs or DEGs. **B-C:** RT-qPCR and western blot were used to detect differences in the expression of EIF4A3, EIF2B1, MNAT1, SNRNP70, and UBE2D1 in serum from the chronic HCV, HCV, and Ctrl groups (N=4)

Interestingly, the present study found that the expression of HSPA4 in the serum of the chronic HCV group was significantly higher than that of the HCV group. The function of HSPA4 in the HCV lifecycle is currently

unknown. Combined with previous studies, we believe that HSPA4 is most likely the biomarker that exacerbates HCV pathogenicity. COPS5 is an important component of the COP9 complex, and plays a key role in the

regulation of protein degradation, signaling and gene expression, among other processes [43, 44]. Previous studies have demonstrated that COPS5 is significantly positively associated with HCV infection and is over-expressed in HCC, which facilitates the progression of HCV-associated HCC in both cellular and animal studies [45]. Interestingly, we found that COPS5 was lowly expressed in the serum of a population with previous HCV infection. Therefore, we hypothesized that knock-down of COPS5 might be beneficial for HCV elimination and alleviation of HCV-induced liver injury disease. It was demonstrated that HCV core protein induced spontaneous HCC through c-Jun/AP-1 signaling [46]. Moreover, COPS5 enhances the activity of the AP-1 transcription factor by interacting with c-Jun, thereby affecting gene expression [44, 47]. Therefore, we believe that HCV may exacerbate liver injury disease through COPS5/c-Jun/AP-1. Blockade of this signaling may be the key to eliminate the effects of HCV. TCP1 is an essential component of the CCT complex and plays a key role in the proper folding and assembly of nascent proteins, cytoskeleton assembly, and cell division [48, 49]. TCP1 was confirmed to be essential for HCV replication, which is associated with interactions between viral NS5B proteins [50]. Notably, TCP1 was upregulated in the serum of patients in the chronic HCV group. These previous studies have highlighted the reliability of the present findings, and the findings of this study provide unlimited possibilities for future mechanistic studies of HCV infection and identification of therapeutic targets.

Notably, the combined analysis of proteomics and transcriptomics revealed interactions between POU5F1 and MNAT1, RNF126, UBE2D1 and UFL1, ETV6, FHIT and ALDH2, and SIK1 and PRKACA. The findings refine the HCV-associated molecular regulatory network and make up for the shortcomings of single proteomics/transcriptomics. The mechanisms underlying these relationships in HCV infection and pathogenesis have not been elucidated. However, based on the known functions of these DEPs/DEGs, it is possible to speculate on their role in HCV infection and pathogenesis. The POU5F1 protein, also known as OCT-4, is a key transcription factor that plays an important role in maintaining the self-renewal and differentiation potential of pluripotent stem cells [51, 52]. HCV core proteins can promote hepatic fibrosis [53] and the cell cycle in HCC by upregulating POU5F1 expression [54]. Notably, we found that POU5F1 was highly expressed in HCV serum and interacted with MNAT1. Interestingly, MNAT1 stabilizes the cell cycle protein H-CDK7 complex, which facilitates the cell cycle [55], and the present study confirmed that MNAT1 is highly expressed in HCV serum. Combined with these studies, we hypothesized that HCV core protein-induced HCC cell cycle is mediated by the interaction between

POU5F1 and MNAT1. In addition, we found that there was an interaction between RNF126 and MNAT1, and that RNF126 was lowly expressed in HCV serum. As one of the E3 ubiquitin-protein ligases, low expression of RNF126 might also contribute to the increased expression of MNAT1.

However, there are still more questions to be addressed in this study. The main limitation of this study is the small sample size ($n = 4$), which will have an impact on the statistical power and representativeness of the findings. Small sample size may limit the general applicability of the findings and may have resulted in some potential biological differences not being effectively detected. Additionally, small sample sizes increase the likelihood that results will be affected by inter-individual. This study is a preliminary exploratory work and the conclusions need to be validated in a large sample cohort. Future studies should incorporate larger sample sizes to minimize bias and provide a more comprehensive understanding of the molecular mechanisms of HCV. Although, this study verified the differential expression of some DEPs/DEGs in clinical samples. Their mechanisms in HCV infection and pathogenesis still need to be validated using *in vivo* and *in vitro* experiments. In conclusion, this study is the first to combine proteomics and transcriptomics to identify molecular features of serum from patients with hepatitis C, and to reveal possible molecular mechanisms of HCV infection and pathogenesis. The findings will provide a reference and potential biomarker for hepatitis C treatment and contribute to HCV-related basic research.

Supplementary Information

The online version contains supplementary material available at <https://doi.org/10.1186/s12985-025-02690-1>.

Supplementary Material 1
Supplementary Material 2
Supplementary Material 3
Supplementary Material 4
Supplementary Material 5
Supplementary Material 6
Supplementary Material 7
Supplementary Material 8
Supplementary Material 9
Supplementary Material 10
Supplementary Material 11

Author contributions

J.W., A.X., R.T., and W.Y. conceived and designed the experiments; J.W., A.X., M.T., S.Y., and Y.S., J.D. performed the experiments; J.W. and A.X. analyzed the data; M.T. and S.Y. contribute to resources and data curation; J.W. and A.X. contribute to writing-Original Draft; M.T., S.Y., Y.S., J.D., R.T., and W.Y. contribute to writing-Review & Editing. All authors have read and agreed to the published version of the manuscript.

Funding

1. The Yunnan Provincial Department of Science and Technology and Kunming Medical University's Joint Special Funding for Applied Basic Research (Grant No. 202101AY070001-250).
2. The Yunnan Provincial Department of Science and Technology and Kunming Medical University's Joint Special Funding for Applied Basic Research (Grant No. 202401AY070001-113).

Data availability

The data supporting the results of this study can be obtained from the author upon reasonable request.

Declarations

Ethical approval

The Ethics Committee of the First People's Hospital of Yunnan Province and the subjects approved this study (Approval No. 2020KYS112), and the subjects signed an informed consent form.

Consent for publication

All subjects consented to the publication of this study.

Competing interests

The authors declare no competing interests.

Received: 2 December 2024 / Accepted: 3 March 2025

Published online: 13 March 2025

References

1. Hepatitis C [EB/OL]. <https://www.who.int/news-room/fact-sheets/detail/hepatitis-c>
2. Updated recommendations on treatment of adolescents and children with chronic HCV infection, and HCV simplified service delivery and diagnostics [EB/OL]. <https://www.who.int/publications/i/item/9789240052734>
3. Castaneda D, Gonzalez AJ, Alomari M, et al. From hepatitis A to E: A critical review of viral hepatitis [J]. *World J Gastroenterol*. 2021;27(16):1691–715.
4. Wedemeyer H, Wiegand J, Cornberg M, et al. Polyethylene glycol-interferon: current status in hepatitis C virus therapy [J]. *J Gastroenterol Hepatol*. 2002;17(Suppl 3):S344–50.
5. Zhang X. Direct anti-HCV agents [J]. *Acta Pharm Sin B*. 2016;6(1):26–31.
6. Di Marco L, La Mantia C, Di Marco V. Hepatitis C. Standard of treatment and what to do for global Elimination [J]. *Viruses*, 2022, 14(3).
7. Fabrizi F, Tripodi F, Cerutti R et al. Recent information on Pan-Genotypic Direct-Acting antiviral agents for HCV in chronic kidney Disease [J]. *Viruses*, 2022, 14(11).
8. Marshall AD, Willing AR, Kairouz A, et al. Direct-acting antiviral therapies for hepatitis C infection: global registration, reimbursement, and restrictions [J]. *Lancet Gastroenterol Hepatol*. 2024;9(4):366–82.
9. Huang CF, Awad MH, Gal-Tanamy M, et al. Unmet needs in the post-direct-acting antivirals era: the risk and molecular mechanisms of hepatocellular carcinoma after hepatitis C virus eradication [J]. *Clin Mol Hepatol*. 2024;30(3):326–44.
10. Maekawa S, Takano S, Enomoto N. Risk of hepatocellular carcinoma after viral clearance achieved by DAA treatment [J]. *J Formos Med Assoc*. 2024;123(11):1124–30.
11. Celsa C, Stornello C, Giuffrida P, et al. Direct-acting antiviral agents and risk of hepatocellular carcinoma: critical appraisal of the evidence [J]. *Ann Hepatol*. 2022;27:100568.
12. Pelaia TM, Shojaei M, Mclean AS. The role of transcriptomics in redefining critical illness [J]. *Crit Care*. 2023;27(1):89.
13. Cui M, Cheng C, Zhang L. High-throughput proteomics: a methodological mini-review [J]. *Lab Invest*. 2022;102(11):1170–81.
14. Mazouz S, Salinas E, Bédard N, et al. Differential immune transcriptomic profiles between vaccinated and resolved HCV reinfected subjects [J]. *PLoS Pathog*. 2022;18(11):e1010968.
15. De Giorgi V, Buonaguro L, Worschch A, et al. Molecular signatures associated with HCV-induced hepatocellular carcinoma and liver metastasis [J]. *PLoS ONE*. 2013;8(2):e56153.
16. Fukuhara T, Matsuura Y. Role of miR-122 and lipid metabolism in HCV infection [J]. *J Gastroenterol*. 2013;48(2):169–76.
17. Van Der Ree MH, Van Der Meer AJ, De Bruijne J, et al. Long-term safety and efficacy of microRNA-targeted therapy in chronic hepatitis C patients [J]. *Antiviral Res*. 2014;111:53–9.
18. Janssen HL, Reesink HW, Lawitz EJ, et al. Treatment of HCV infection by targeting microRNA [J]. *N Engl J Med*. 2013;368(18):1685–94.
19. Lussignol M, Kopp M, Molloy K, et al. Proteomics of HCV virions reveals an essential role for the nucleoporin Nup98 in virus morphogenesis [J]. *Proc Natl Acad Sci U S A*. 2016;113(9):2484–9.
20. Liu S, Zhao T, Song B, et al. Comparative proteomics reveals important Viral-Host interactions in HCV-Infected human liver Cells [J]. *PLoS ONE*. 2016;11(1):e0147991.
21. Cento V, Nguyen THT, Di Carlo D, et al. Improvement of ALT decay kinetics by all-oral HCV treatment: role of NS5A inhibitors and differences with IFN-based regimens [J]. *PLoS ONE*. 2017;12(5):e0177352.
22. Wilfret DA, Walker J, Adkison KK, et al. Safety, tolerability, pharmacokinetics, and antiviral activity of GSK2336805, an inhibitor of hepatitis C virus (HCV) NS5A, in healthy subjects and subjects chronically infected with HCV genotype 1 [J]. *Antimicrob Agents Chemother*. 2013;57(10):5037–44.
23. Mohammadi-Shemirani P, Sood T, Paré G. From 'omics to Multi-omics technologies: the discovery of novel causal Mediators [J]. *Curr Atheroscler Rep*. 2023;25(2):55–65.
24. Selvarajoo K, Maurer-Stroh S. Towards multi-omics synthetic data integration [J]. *Brief Bioinform*, 2024, 25(3).
25. Zhi CM, a J Z G Z B. Z. Guidelines for the prevention and treatment of hepatitis C (2019 version) [J]. 2019, 27: 962–79.
26. Chinese Society of Hepatology C M A, Chinese Society of Infectious, Diseases CMA, Wei L, et al. Guideline for the prevention and treatment of hepatitis C (2022 version) [J]. *Chin J Clin Infect Dis*. 2022;15(06):428–47.
27. Love MI, Huber W, Anders S. Moderated Estimation of fold change and dispersion for RNA-seq data with DESeq2 [J]. *Genome Biol*. 2014;15(12):550.
28. Subramanian A, Tamayo P, Mootha VK, et al. Gene set enrichment analysis: a knowledge-based approach for interpreting genome-wide expression profiles [J]. *Proc Natl Acad Sci U S A*. 2005;102(43):15545–50.
29. Aleksander SA, Balhoff J, Carbon S et al. The gene ontology knowledgebase in 2023 [J]. *Genetics*, 2023, 224(1).
30. Kanehisa M, Goto S. KEGG: Kyoto encyclopedia of genes and genomes [J]. *Nucleic Acids Res*. 2000;28(1):27–30.
31. Wang L, Wang S, Li W. RSeQC: quality control of RNA-seq experiments [J]. *Bioinformatics*. 2012;28(16):2184–5.
32. Chen S, Zhou Y, Chen Y, et al. Fastp: an ultra-fast all-in-one FASTQ preprocessor [J]. *Bioinformatics*. 2018;34(17):i884–90.
33. Kim D, Langmead B, Salzberg SL. HISAT: a fast spliced aligner with low memory requirements [J]. *Nat Methods*. 2015;12(4):357–60.
34. Liao Y, Smyth GK, Shi W. FeatureCounts: an efficient general purpose program for assigning sequence reads to genomic features [J]. *Bioinformatics*. 2014;30(7):923–30.
35. Livak KJ, Schmittgen TD. Analysis of relative gene expression data using real-time quantitative PCR and the 2(-Delta Delta C(T)) Method [J]. *Methods*. 2001;25(4):402–8.
36. Zou C, Tan H, Zeng J, et al. Hepatitis C virus nonstructural protein 4B induces lipogenesis via the Hippo pathway [J]. *Arch Virol*. 2023;168(4):113.
37. Majeau N, Bolduc M, Duvignaud JB, et al. Effect of cAMP-dependent protein kinase A (PKA) on HCV nucleocapsid assembly and degradation [J]. *Biochem Cell Biol*. 2007;85(1):78–87.
38. Bode JG, Brenndörfer ED, Karthe J, et al. Interplay between host cell and hepatitis C virus in regulating viral replication [J]. *Biol Chem*. 2009;390(10):1013–32.
39. Yang J, Wu X, You J. Unveiling the potential of HSPA4: a comprehensive pan-cancer analysis of HSPA4 in diagnosis, prognosis, and immunotherapy [J]. *Aging*. 2024;16(3):2517–41.
40. Lubkowska A, Pluta W, Strońska A et al. Role of heat shock proteins (HSP70 and HSP90) in viral Infection [J]. *Int J Mol Sci*, 2021, 22(17).
41. Khachatoorian R, Riahi R, Ganapathy E, et al. Allosteric heat shock protein 70 inhibitors block hepatitis C virus assembly [J]. *Int J Antimicrob Agents*. 2016;47(4):289–96.
42. Toraih EA, Alrefai HG, Hussein MH, et al. Overexpression of heat shock protein HSP90AA1 and translocase of the outer mitochondrial membrane TOM34 in HCV-induced hepatocellular carcinoma: A pilot study [J]. *Clin Biochem*. 2019;63:10–7.

43. Yuan C, Wang D, Liu G, et al. Jab1/Cops5: a promising target for cancer diagnosis and therapy[J]. *Int J Clin Oncol*. 2021;26(7):1159–69.
44. Yang Y, Song R, Gao Y, et al. Regulatory mechanisms and therapeutic potential of JAB1 in neurological development and disorders[J]. *Mol Med*. 2023;29(1):80.
45. Hsu MC, Huang CC, Chang HC, et al. Overexpression of Jab1 in hepatocellular carcinoma and its inhibition by peroxisome proliferator-activated receptor[gamma] ligands in vitro and in vivo[J]. *Clin Cancer Res*. 2008;14(13):4045–52.
46. Machida K, Tsukamoto H, Liu JC, et al. c-Jun mediates hepatitis C virus hepatocarcinogenesis through signal transducer and activator of transcription 3 and nitric oxide-dependent impairment of oxidative DNA repair[J]. *Hepatology*. 2010;52(2):480–92.
47. Chamovitz DA, Segal D. JAB1/CAN1 and the COP9 signalosome. A complex situation[J]. *EMBO Rep*. 2001;2(2):96–101.
48. Willison KR. The structure and evolution of eukaryotic chaperonin-containing TCP-1 and its mechanism that folds actin into a protein spring[J]. *Biochem J*. 2018;475(19):3009–34.
49. Ghozlan H, Cox A, Nierenberg D, et al. The tricky business of protein folding in health and disease[J]. *Front Cell Dev Biol*. 2022;10:906530.
50. Inoue Y, Aizaki H, Hara H, et al. Chaperonin TRiC/CCT participates in replication of hepatitis C virus genome via interaction with the viral NS5B protein[J]. *Virology*. 2011;410(1):38–47.
51. Patel I, Parchem RJ. Regulation of Oct4 in stem cells and neural crest cells[J]. *Birth Defects Res*. 2022;114(16):983–1002.
52. Mohiuddin IS, Wei SJ, Kang MH. Role of OCT4 in cancer stem-like cells and chemotherapy resistance[J]. *Biochim Biophys Acta Mol Basis Dis*. 2020;1866(4):165432.
53. Li W, Duan X, Zhu C, et al. Hepatitis B and hepatitis C virus infection promote liver fibrogenesis through a TGF- β 1-induced OCT4/Nanog pathway[J]. *J Immunol*. 2022;208(3):672–84.
54. Zhou JJ, Meng Z, Zhou Y, et al. Hepatitis C virus core protein regulates OCT4 expression and promotes cell cycle progression in hepatocellular carcinoma[J]. *Oncol Rep*. 2016;36(1):582–8.
55. Eki T, Okumura K, Abe M, et al. Mapping of the human genes encoding Cyclin H (CCNH) and the CDK-activating kinase (CAK) assembly factor MAT1 (MNAT1) to chromosome bands 5q13.3-q14 and 14q23, respectively[J]. *Genomics*. 1998;47(1):115–20.

Publisher's note

Springer Nature remains neutral with regard to jurisdictional claims in published maps and institutional affiliations.